International Journal of Computer Information Systems and Industrial Management Applications
ISSN 2150-7988 Volume 18(5s) 2026 pp. 362-375
https://doi.org/10.70917/ijcisim-2026-2716
Article

WASTE BAOBAB AND TAMARIND LEAVES OF DHOFAR AS ADSORBENTS FOR PROPIONIC ACID REMOVAL FROM ITS AQUEOUS SOLUTION: ADSORPTION KINETIC MODELLING

Sivamani Selvaraju[2], B. S. Naveen Prasad[1], Saikat Banerjee[1], Raja Thiruvengadam[1]*

[1] College of Engineering and Technology, University of Technology and Applied Sciences (UTAS), Salalah, Oman.
[2] Department of Bioengineering, Saveetha School of Engineering, SIMATS, Saveetha University, Chennai, Tamil Nadu, India.
Corresponding Author: Sivamani Selvaraju, sivamani.selvaraju@utas.edu.om; sivmansel@gmail.com

Abstract: The adsorption kinetics of propionic acid from its aqueous solution onto raw and activated baobab (RB, AB) and tamarind (RT, AT) biosorbents of Dhofar were systematically investigated to evaluate the influence of biosorbent activation on adsorption performance and mechanism. Experimental data were analyzed using linear forms of five kinetic models, including pseudo-first order (PFO), pseudo-second order (PSO), Elovich (EV), intra-particle diffusion (IPD), and Boyd (BY) models. Model performance was assessed through comprehensive error analytical parameters, including sum of squared errors (SSE), mean squared sum of errors (MSSE), standard error (SE), average absolute relative deviation (AARD), and determination coefficient (R2). The results revealed that adsorption capacity and rate were significantly enhanced after chemical activation, with AB showing the highest overall performance followed by RB, AT, and RT. Kinetic analysis indicated that the pseudo-second-order model best described the adsorption process for all biosorbents, supported by the highest R^2 values and the lowest error statistics, suggesting that chemisorption is the dominant mechanism controlling propionic acid uptake. The Elovich model further confirmed adsorption on heterogeneous surfaces, while IPD and Boyd models indicated that both film diffusion and intraparticle diffusion contributed to the overall rate, without being sole rate-limiting steps. Error analysis validated the robustness and reliability of the PSO model in predicting adsorption behavior. Overall, the study demonstrates that waste-derived baobab and tamarind biosorbents, particularly in activated form, are effective, low-cost, and sustainable materials for propionic acid removal from aqueous solutions, offering promising applications in wastewater treatment.
Keywords: Adsorption, Propionic acid, Baobab, Tamarind, Kinetics, Mechanism

1. INTRODUCTION

Wastewater is generated from a variety of domestic, industrial, and agricultural activities and contains numerous physical, chemical, and biological pollutants. When discharged into the environment without adequate treatment, it can cause substantial damage to both aquatic and terrestrial ecosystems [1]. The decomposition of organic matter present in wastewater consumes dissolved oxygen in receiving water bodies, resulting in oxygen depletion that can endanger fish and other aquatic organisms [2]. In addition, wastewater may contain toxic compounds, excess nutrients, and pathogenic microorganisms that can disturb ecological balance, facilitate disease transmission, and contaminate drinking water supplies, thereby posing serious threats to public health and food security [3,4].

Among the various pollutants found in wastewater, organic acids are frequently encountered, particularly in effluents from food-processing facilities, pharmaceutical manufacturing, textile production, and fermentation-related industries. Compounds such as acetic, formic, lactic, and propionic acids contribute significantly to both chemical

oxygen demand (COD) and biological oxygen demand (BOD) levels [5,6]. Elevated concentrations of these acids can reduce wastewater pH, creating corrosive conditions that negatively affect treatment systems [7]. Such acidic environments may suppress microbial activity, decrease biological treatment performance, and accelerate deterioration of pipelines, reactors, and other infrastructure. Furthermore, organic acids can enhance the dissolution and transport of heavy metals, increasing their bioavailability and toxic impact on living organisms [8,9].

A range of technologies has been developed to remove or mitigate organic acids in wastewater streams [7]. Biological treatment methods, including activated sludge processes and anaerobic digestion, are widely used because they are relatively economical and effective for degrading biodegradable organic compounds. Nevertheless, their performance can be adversely affected by significant pH variations and excessive organic loading [10]. Physicochemical approaches, such as neutralization, membrane-based separation, advanced oxidation techniques, and adsorption, are also commonly applied, particularly for wastewaters containing concentrated or poorly biodegradable organic acids [11]. The choice of an appropriate treatment strategy depends on factors such as wastewater composition, environmental regulations, and overall treatment costs [12,13].

Adsorption has emerged as a promising wastewater treatment technique due to its operational simplicity, adaptability, and high pollutant removal capability. In this process, contaminants are transferred from the liquid phase and retained on the surface of solid materials, including activated carbon, biochar, zeolites, and various modified natural adsorbents [14,15]. Adsorption is especially suitable for treating wastewater containing low to moderate levels of organic acids and is often employed as a polishing step following biological treatment. The process offers several advantages, including minimal formation of harmful byproducts, straightforward operation, and the flexibility to target different contaminants through appropriate adsorbent selection [16,17]. In this regard, the Dhofar region of Oman possesses abundant renewable biomass and naturally occurring mineral resources that remain largely unexplored for environmental remediation purposes [18,19]. Utilizing these locally available materials as adsorbents could provide an environmentally sustainable and economically viable alternative to commercial products while promoting wastewater treatment solutions tailored to regional conditions [20–22].

The performance of adsorption systems is influenced by several operational parameters, including contact time, adsorbent dosage, contaminant concentration, and overall process conditions. Consequently, adsorption kinetic modelling is a key component in the design and optimization of wastewater treatment systems [23,24]. Kinetic models provide insight into adsorption rates, reveal the mechanisms governing pollutant uptake, and help predict system behavior under varying operating conditions [25,26]. Such understanding enables engineers to develop more efficient treatment processes, reduce operational costs, and meet environmental compliance requirements. Therefore, adsorption kinetic analysis is essential for enhancing the effectiveness of adsorption-based treatment technologies and supporting the development of sustainable wastewater management practices [27–30].

Recent studies have demonstrated a variety of adsorption approaches for the removal of propionic acid and other short-chain organic acids using polymeric, carbonaceous, mineral-based, and engineered adsorbent materials [31–33]. The adsorption performance of these materials is strongly influenced by surface chemistry, pore structure, functional groups, and solution conditions such as pH and temperature [34,35]. Polymeric ion-exchange resins have attracted considerable attention for the separation and recovery of carboxylic acids from aqueous and non-aqueous media because of their high selectivity and regeneration potential. Weak-base and strong-base anion exchange resins containing amine functional groups have been reported to effectively adsorb propionic acid through electrostatic interactions, hydrogen bonding, and acid–base mechanisms [33,36]. The adsorption capacity of these materials is often enhanced under conditions where propionic acid exists predominantly in its undissociated form, highlighting the importance of pH control during treatment processes [31].

Carbon-based adsorbents derived from agricultural and industrial wastes have also been widely investigated as low-cost alternatives for organic acid removal [37]. Activated carbons prepared from lignocellulosic biomass generally exhibit high surface areas and well-developed pore networks that facilitate the adsorption of propionic acid molecules. Several studies have reported that adsorption behavior is governed by both physical adsorption within microporous structures and chemical interactions involving oxygen-containing surface functional groups [38,39]. The adsorption process is commonly described using Langmuir and Freundlich isotherm models, indicating the contribution of both homogeneous and heterogeneous adsorption sites [40].

Mineral adsorbents, including natural zeolites, modified clays, and metal oxides, have also shown potential for the removal of short-chain fatty acids from aqueous solutions [41]. Zeolitic materials possess well-defined pore structures and ion-exchange properties that promote the uptake of organic acids through a combination of electrostatic attraction and surface complexation mechanisms. Surface modification of these materials has been shown to improve

adsorption efficiency by increasing hydrophobicity and the availability of active sites [42,43]. Furthermore, studies employing spectroscopic and microscopic characterization techniques have provided valuable insights into the interactions between carboxylic acid molecules and adsorbent surfaces, revealing the importance of hydrogen bonding and surface functionalization in determining adsorption performance [44].

The adsorption of propionic acid has also been investigated in the context of volatile fatty acid recovery from fermentation broths and industrial wastewaters [45]. Research has demonstrated that adsorbent properties, solution chemistry, and operating conditions significantly affect removal efficiency and selectivity. In particular, adsorption performance is strongly dependent on pH, contact time, adsorbent dosage, and initial acid concentration, which influence both mass-transfer processes and adsorption equilibrium [13,46]. These findings emphasize the need for optimized adsorbent design and process conditions to achieve efficient propionic acid removal in practical wastewater treatment applications.

Although numerous studies have examined the adsorption of organic acids and volatile fatty acids on a wide range of adsorbent materials, most investigations have focused primarily on equilibrium characteristics, acid recovery processes, or adsorbent development rather than adsorption kinetics under realistic wastewater conditions [17,33,39]. Furthermore, many studies have been conducted using synthetic solutions under controlled laboratory environments, which may not accurately represent the complexity of actual wastewater systems. The effects of operational parameters on adsorption rates, diffusion mechanisms, and overall process performance remain insufficiently understood, particularly for sustainable and low-cost adsorbents intended for large-scale wastewater treatment applications [47,48].

Therefore, the present study aims to investigate the adsorption kinetics of propionic acid in aqueous systems using a suitable adsorbent under environmentally relevant conditions. By applying kinetic models to experimental adsorption data, the study seeks to identify the dominant adsorption mechanisms and evaluate the influence of key operational parameters on propionic acid removal. The outcomes are expected to contribute to the development of efficient adsorption-based treatment strategies and provide design information for sustainable wastewater treatment systems.

Based on the findings of the literature review and the identified research gaps, this study aims to investigate the removal of propionic acid from aqueous solutions using biosorbents derived from waste baobab and tamarind tree biomass available in the Dhofar region of Oman. The specific objectives of the study are: (i) To prepare and characterize raw and activated biosorbents produced from waste baobab and tamarind tree materials collected in Dhofar; (ii) To evaluate the influence of contact time on the adsorption capacity and removal efficiency of propionic acid from aqueous solutions using the prepared raw and activated biosorbents; and (iii) To assess the adsorption kinetics and elucidate the underlying adsorption mechanisms by applying various kinetic models, including the pseudo-first-order (Lagergren), pseudo-second-order, Elovich, intraparticle diffusion, and Boyd models to the experimental data.

2. MATERIALS AND METHODS:

Materials

All chemicals used in this study were of analytical grade and were utilized without additional purification. Propionic acid (≥99%, Sigma-Aldrich) served as the adsorbate for all adsorption experiments. Distilled water was used for the preparation of solutions and for washing procedures. The raw materials employed for biosorbent production were obtained locally from the Dhofar region of Oman.

Preparation of Adsorbate Solution

A 1.0 M stock solution of propionic acid was prepared by diluting analytical-grade propionic acid with distilled water. Based on the density and purity of the acid, the required volume was accurately measured using a calibrated volumetric pipette and transferred into a 500 mL volumetric flask. Distilled water was then added gradually to reach the desired final volume. The resulting solution was thoroughly mixed to ensure complete homogeneity and subsequently used as the stock adsorbate solution for all experiments. Working solutions of the required concentrations were prepared by appropriate dilution of the stock solution with distilled water prior to each adsorption test.

Preparation of Raw and Activated Baobab and Tamarind Biosorbents

Raw biosorbents were prepared from the dried leaves of baobab (Adansonia digitata) and tamarind (Tamarindus indica) collected from Wadi Hanna and Taqah, respectively, in the Dhofar Governorate of Oman. The collected leaves

were initially cleaned to remove dust, dirt, and other surface contaminants before being sun-dried for five days to eliminate moisture. After drying, unwanted materials such as petioles, bark fragments, and other foreign matter were manually removed [20,49]. The cleaned leaves were ground using a laboratory blender to obtain a fine powder. The powdered materials were subsequently sieved through a 1.0 mm mesh screen, and the fractions passing through the sieve were collected as the raw biosorbents. These materials were stored in airtight containers until further use, while the retained coarse particles were discarded.

Chemical activation of the biosorbents was performed using sulfuric acid. For each biomass type, 25 g of the raw biosorbent was mixed with 75 mL of 4.0 M sulfuric acid to form a uniform paste. The mixture was allowed to stand for 1 h to facilitate the activation process [49]. Following activation, the materials were repeatedly washed with distilled water until the wash water reached a neutral pH, indicating complete removal of residual acid. The activated biosorbents were then sun-dried for five days to remove moisture. After drying, the final masses of the activated baobab and tamarind biosorbents were recorded and used in subsequent adsorption studies., as given in Equation (1).

$$\text{Yield \%} = \frac{Mass\ of\ activated\ biosorbent}{Mass\ of\ raw\ powder} \times 100 \quad (1)$$

Effect of Contact Time on Propionic Acid Adsorption

Batch adsorption experiments were conducted to evaluate the influence of contact time on the adsorption of propionic acid using raw baobab (RB), activated baobab (AB), raw tamarind (RT), and activated tamarind (AT) biosorbents. Working solutions of propionic acid were prepared by diluting the stock solution with distilled water. Aliquots of 50 mL were transferred into separate 250 mL conical flasks [49]

A fixed biosorbent dosage of 0.1 g was added to each flask. The suspensions were agitated using a magnetic stirrer at 150 rpm under ambient laboratory conditions (approximately 25 °C). Samples were withdrawn at predetermined time intervals of 2 min. At each sampling point, 10 mL of the solution was collected and filtered through Whatman No. 42 filter paper to remove suspended biosorbent particles. The filtrate was subsequently analyzed for residual propionic acid concentration using a UV–Visible spectrophotometer. The adsorption experiments continued until equilibrium was attained, as indicated by negligible changes in propionic acid concentration with time. All experiments were conducted in triplicate to ensure the reliability and reproducibility of the results. The adsorption capacity at any contact time, (q_t), was calculated using Equation (2):

$$q_t = \frac{(C_0 - C_t)\,V}{m} \quad (2)$$

where, C_0 and C_t are the initial and time-dependent concentrations of the acid (mol.L^{-1}), V is the volume of the solution (L), and m is the mass of the biosorbent (g). This procedure enabled the evaluation of adsorption kinetics and comparison of the adsorption performance of raw and activated biosorbents. Kinetic studies were carried out by monitoring the variation in propionic acid concentration as a function of contact time.

Analytical method for residual acetic acid in aqueous solution:

The concentration of propionic acid remaining in solution after adsorption was determined using a UV–Visible spectrophotometer (Shimadzu UV-1800). Prior to analysis, all samples were filtered through Whatman No. 42 filter paper to eliminate suspended biosorbent particles [49]. A calibration curve was established using standard propionic acid solutions of known concentrations prepared from the stock solution. The absorbance of each standard was measured in triplicate, and the corresponding calibration plot was constructed. A strong linear relationship between absorbance and concentration was obtained, with a correlation coefficient (R^2) exceeding 0.995. The absorbance values of the adsorption samples were measured under identical conditions, and their concentrations were determined from the calibration curve. All analyses were performed at room temperature (approximately 25 °C). Distilled water blanks were analyzed periodically to account for background absorbance, and all measurements were corrected accordingly to ensure analytical accuracy.

Kinetic models used in the adsorption of acetic acid from its aqueous solution using raw and activated biosorbents from waste baobab and tamarind trees in Dhofar:

Pseudo-first order (PFO) model

The pseudo-first order (Lagergren) kinetic model assumes that the adsorption rate is proportional to the number of unoccupied sites on the biosorbent surface and is mainly applicable to physical adsorption at the initial stage, as shown in Equation (3):

$$\log(q_e - q_t) = \log q_e - \left(\frac{K_1}{2.303}\right) t \qquad (3)$$

where, q_e is equilibrium adsorption capacity (mol.g^{-1}), K_1 is pseudo-first order rate constant (min^{-1}), and t is time (min) [49].

Pseudo-Second order model

The pseudo-second-order kinetic model assumes that the adsorption rate is controlled by chemical interactions between the adsorbate and the biosorbent and depends on the availability of active sites, as shown in Equation (4):

$$\frac{t}{q_t} = \frac{1}{K_2 {q_e}^2} + \frac{1}{q_e}\, t \qquad (4)$$

where, K_2 is pseudo-second order rate constant (mol^{-1}.g^{-1}.min^{-1}) [49].

Elovich model

The Elovich model is used to describe adsorption processes on energetically heterogeneous surfaces where the activation energies vary for different adsorption sites. The model is represented by Equation (5):

$$q_t = \frac{ln(\alpha\beta)}{\beta} + \frac{ln\, t}{\beta} \qquad (5)$$

$$\ln t = q_t\beta - ln(\alpha\beta)$$

where, α is initial adsorbate adsorption rate (mol·g^{-1}·min^{-1}), β is adsorption constant (g·mol^{-1}), Initial adsorption rate (α) and adsorption constant (β) can be evaluated from a linear plot of qt versus ln t [49].

Intra-particle diffusion model:

The intra-particle diffusion model (Weber-Morris model) is used to identify whether diffusion within the pores of the adsorbent is the rate-limiting step in the adsorption process. The model is expressed in Equation (6) as:

$$q_t = K_{IPD}\, t^{1/2} + C \qquad (6)$$

where K_{IPD} is intra-particle diffusion constant (mol·g^{-1}.min$^{-1/2}$), C = Thickness of boundary layer (mol.g^{-1}) [49].

Boyd model

The Boyd model is used to determine the rate-controlling step in adsorption processes, distinguishing whether external mass transfer or internal diffusion is the slow step, as shown in Equation (7):

$$B_t = Bt = -0.4977 - \ln\left(1 - \frac{q_t}{q_e}\right) \qquad (7)$$

where B is Boyd rate constant [49].

Error analytical parameters for kinetic modelling of adsorption of acetic acid using raw and activated baobab and tamarind biosorbents:

In adsorption kinetic studies, statistical error analysis plays a crucial role in assessing the suitability, accuracy, and predictive performance of kinetic models. For the adsorption of propionic acid onto raw and activated baobab and tamarind biosorbents, various error functions are employed to measure the differences between experimentally determined adsorption capacities and those predicted by kinetic models. These statistical indicators provide valuable information regarding model fit, reliability, and predictive accuracy, thereby facilitating the identification of the kinetic model that most effectively describes the adsorption process [49].

Residual or error sum of squares (absolute)

Residual or error sum of squares (SSE), as given in Equation (11), measures the total squared deviation between experimental observations and model predictions. It directly reflects the overall discrepancy of the kinetic model from experimental data. Lower SSE values indicate a better fit of the kinetic model to experimental adsorption data.

$$SSE = \sum_{i=1}^{n}(Y_o - Y_p)^2 \qquad (11)$$

where Yo and Yp are experimental and predicted values of adsorption capacity [49].

Error variance of the estimate (MSSE)

Error variance of the estimate (MSSE), as given in Equation (12), represents the average squared error per degree of freedom and accounts for the number of fitted parameters in the model. It provides a normalized measure of model error. Smaller MSSE values signify higher model precision and reliability.

$$MSSE = \frac{SSE}{n-p} \qquad (12)$$

where n is number of experimental data considered for analysis, and p is number of model parameters [49].

Standard error of the estimate (SE)

Standard error of the estimate (SE), as given in Equation (13), indicates the dispersion of experimental data points around the predicted values and is expressed in the same units as the response variable. Lower SE values suggest closer agreement between experimental and predicted adsorption kinetics [49].

$$SE = \sqrt{\frac{SSE}{n-p}} \qquad (13)$$

Absolute average deviation (AARD)

Absolute average deviation (AARD), as given in Equation (14), evaluates the average relative deviation between experimental and predicted values, making it particularly useful for comparing models across different data scales. Lower AARD values (typically < 10%) indicate excellent model performance [49].

$$Absolute\ average\ deviation\ AARD = \frac{1}{n}\sum_{i=1}^{n}\frac{|Y_o - Y_p|}{Y_o} \qquad (14)$$

Determination coefficient (R2)

Determination coefficient (R2), as given in Equation (15), quantifies the proportion of variance in the experimental data explained by the kinetic model. It is a primary indicator of goodness-of-fit. R^2 values closer to 1 indicate superior model accuracy [49].

$$Determination\ coefficient\ R^2 = \frac{\sum_{i=1}^{n}(Y_p - \bar{Y}_p)^2}{\sum_{i=1}^{n}(Y_p - \bar{Y}_p)^2 + \sum_{i=1}^{n}(Y_o - Y)^2} \qquad (15)$$

3. RESULTS AND DISCUSSION:

Biosorbent yield:

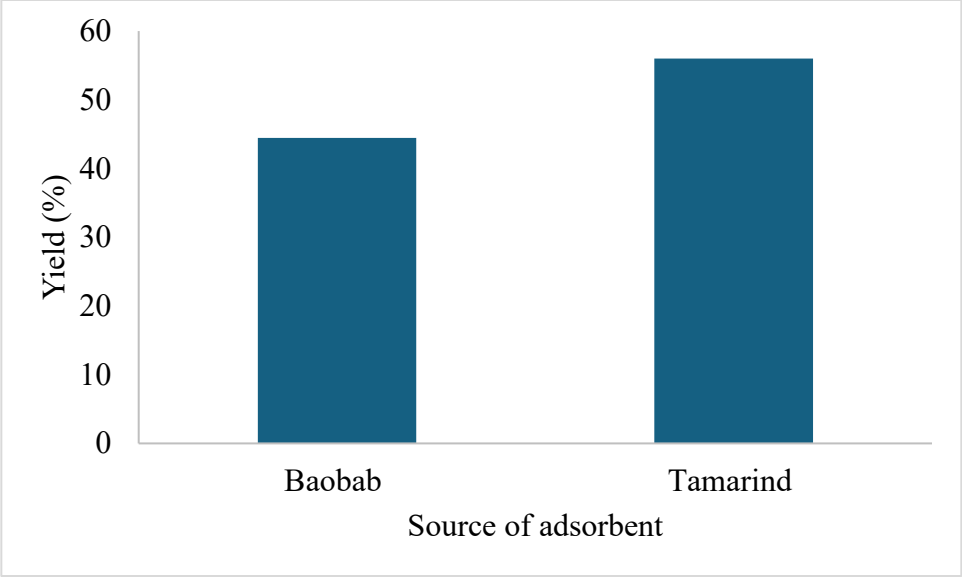

Figure 1. Yield of activated biosorbents from raw powder for baobab and tamarind

Figure 1 illustrates the activation yields obtained from baobab and tamarind biosorbents. The activation yield represents the proportion of activated biosorbent recovered after the activation process relative to the initial mass of raw biomass, expressed as a percentage. The results show that activation of 25 g of raw baobab powder produced 11.11 g of activated biosorbent, corresponding to a yield of 44.44%. This indicates that approximately half of the original biomass mass was retained after activation, reflecting a moderate conversion efficiency. In contrast, activation of 25 g of raw tamarind powder yielded 14.00 g of activated biosorbent, equivalent to a recovery of 56.00%. The higher yield obtained from tamarind suggests greater retention of biomass during the activation process and indicates a more efficient conversion to activated biosorbent compared with baobab. Overall, the results demonstrate that tamarind biomass provided a higher activated biosorbent yield than baobab under the same activation conditions, making it a potentially more favorable precursor for biosorbent production.

Effect of contact time on adsorption capacity for acetic acid removal from its aqueous solution using raw and activated biosorbents from waste baobab and tamarind trees:

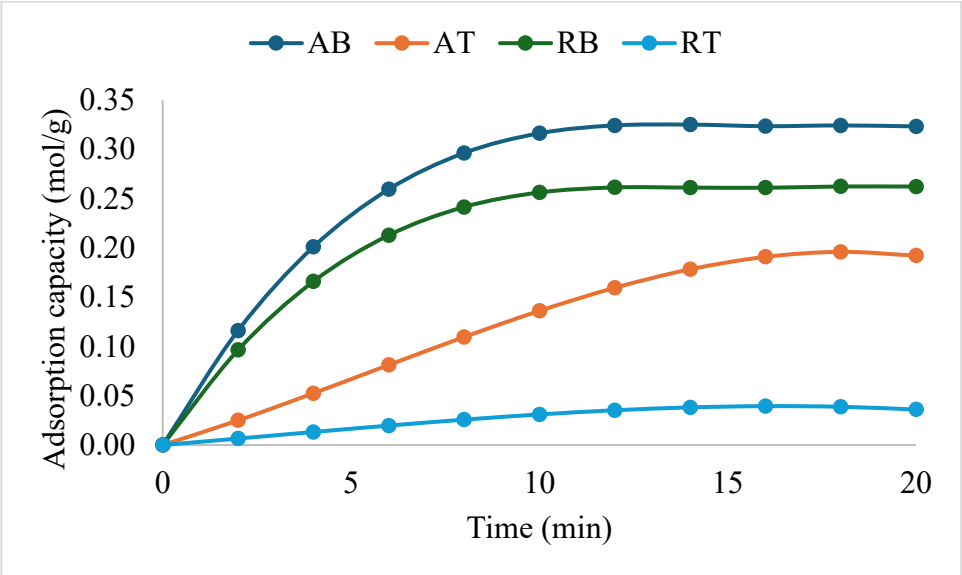

Figure 2. Effect of contact time on adsorption capacity for propionic acid removal from its aqueous solution using raw and activated biosorbents from waste baobab and tamarind trees (AB: Activated baobab, AT: Activated tamarind, RB: Raw baobab, RT: Raw tamarind)

Figure 2 presents the variation of adsorption capacity with contact time for propionic acid adsorption onto activated baobab (AB), activated tamarind (AT), raw baobab (RB), and raw tamarind (RT) biosorbents. In all cases, adsorption capacity increased rapidly during the initial stages of the process, followed by a gradual approach to equilibrium. This trend is characteristic of adsorption systems in which a large number of vacant adsorption sites are initially available, allowing rapid uptake of adsorbate molecules. As contact time increases, the number of available active sites decreases and adsorption slows until equilibrium is reached.

Among the four biosorbents, activated baobab (AB) exhibited the highest adsorption capacity throughout the experimental period. The adsorption capacity increased sharply from 0 mol g^{-1} at the start of the experiment to approximately 0.20 mol g^{-1} within the first 4 min, indicating rapid adsorption kinetics. Thereafter, the rate of adsorption gradually decreased, reaching an equilibrium value of approximately 0.32 mol g^{-1} after 12 min. Beyond this point, no significant increase in adsorption capacity was observed, suggesting complete occupation of the available adsorption sites. The superior performance of AB can be attributed to the sulfuric acid activation process, which likely enhanced surface area, pore development, and the number of surface functional groups available for interaction with propionic acid molecules.

Raw baobab (RB) demonstrated the second-highest adsorption capacity. Similar to AB, adsorption occurred rapidly during the initial stages, reaching approximately 0.17 mol g^{-1} after 4 min. The adsorption capacity continued to increase gradually and attained equilibrium at approximately 0.26 mol g^{-1} after 12–14 min. Although the adsorption behavior of RB followed the same trend as AB, the lower equilibrium capacity indicates that activation significantly improved the adsorption characteristics of baobab biomass. The difference between AB and RB suggests that chemical activation generated additional active sites and improved accessibility of the internal pore structure.

Activated tamarind (AT) exhibited moderate adsorption performance. The adsorption capacity increased steadily throughout the experimental period, reaching approximately 0.19 mol g^{-1} after 18 min. Unlike AB and RB, equilibrium was achieved more slowly, indicating that adsorption kinetics on AT were less favorable. The slower adsorption rate may be associated with differences in pore structure, surface chemistry, or distribution of functional groups compared with baobab-derived biosorbents. Nevertheless, activation substantially enhanced the adsorption capacity of tamarind biomass when compared with its raw counterpart.

Raw tamarind (RT) displayed the lowest adsorption capacity among all biosorbents. The adsorption process proceeded slowly, reaching a maximum capacity of only about 0.04 mol g^{-1} after 16–18 min. The limited adsorption performance of RT suggests a relatively low number of active sites and a less developed pore structure. The small increase in adsorption capacity over time indicates weak interactions between propionic acid molecules and the raw tamarind surface. This result highlights the importance of chemical activation in improving the adsorption efficiency of tamarind biomass.

Comparison of the equilibrium adsorption capacities reveals the following order of adsorption performance, AB > RB > AT > RT, with equilibrium capacities of approximately 0.32, 0.26, 0.19, and 0.04 mol g^{-1}, respectively. Activated baobab achieved an adsorption capacity approximately 23% higher than raw baobab and nearly eight times greater than raw tamarind. These results clearly demonstrate the beneficial effect of sulfuric acid activation on biosorbent performance and indicate that baobab biomass possesses more favorable adsorption characteristics than tamarind biomass for propionic acid removal.

The adsorption profiles also suggest the occurrence of a two-stage adsorption mechanism. The initial rapid adsorption phase can be attributed to external surface adsorption and film diffusion, where propionic acid molecules quickly occupy readily accessible active sites. The subsequent slower phase is likely controlled by intraparticle diffusion and gradual penetration of adsorbate molecules into the internal pores of the biosorbent. The attainment of equilibrium after approximately 12–18 min indicates relatively fast adsorption kinetics, which is advantageous for practical wastewater treatment applications because shorter contact times reduce reactor volume requirements and operational costs.

Overall, the results demonstrate that activated baobab is the most effective biosorbent for propionic acid removal, exhibiting both the highest adsorption capacity and the fastest adsorption rate. The findings further confirm that chemical activation significantly enhances adsorption performance by improving the physicochemical properties of the biosorbent, making activated baobab a promising low-cost adsorbent for the treatment of propionic acid-containing wastewater.

Kinetic models used in the adsorption of acetic acid using raw and activated baobab and tamarind biosorbents:

Table 1 shows the kinetic model parameters for the adsorption of propionic acid onto raw and activated baobab and tamarind biosorbents, obtained by fitting the experimental data to various kinetic and diffusion models. To better understand the adsorption behavior of propionic acid on raw and activated baobab (RB and AB) and tamarind (RT and AT) biosorbents, the experimental data were analyzed using pseudo-first-order (PFO), pseudo-second-order (PSO), Elovich (EV), intraparticle diffusion (IPD), and Boyd (BY) kinetic models. The estimated kinetic parameters obtained from each model are presented in Table X. These parameters provide valuable information regarding adsorption rate, adsorption capacity, diffusion characteristics, and the dominant mechanisms controlling the adsorption process.

Table 1. Model parameters in the adsorption kinetics of propionic acid using raw and activated baobab and tamarind biosorbents

Model	Parameters	AB	AT	RB	RT
PFO	K1 (min-1)	0.362	0.121	0.377	0.171
	qe (mol/g)	0.426	0.211	0.348	0.043
PSO	K2 (mol.L-1min-1)	0.738	0.021	0.979	0.657
	qe (mol/g)	0.394	0.837	0315	0.081
EV	(mol·g−1·min−1)	0.180	0.044	0.152	0.010
	(g·mol−1)	9.908	11.56	12.50	61.30
IPD	KIPD (mol·g−1.min-1/2)	11.84	18.46	14.70	93.45
	C (mol.g-1)	-0.133	0.674	-0.156	0.177
BY	B (min-1)	0.259	0.056	0.273	0.094

The pseudo-first-order model assumes that the adsorption rate is proportional to the number of unoccupied adsorption sites. The calculated adsorption capacities ((qe)) obtained from this model were 0.426, 0.211, 0.348, and 0.043 mol g^{-1} for AB, AT, RB, and RT, respectively. Among all biosorbents, activated baobab exhibited the highest equilibrium adsorption capacity, indicating its superior affinity toward propionic acid molecules. The corresponding rate constant ((K1)) for AB was 0.362 min^{-1}, which was considerably higher than those of AT (0.121 min^{-1}) and RT (0.171 min^{-1}), suggesting a faster adsorption rate. Raw baobab also showed a relatively high rate constant (0.377 min^{-1}), indicating rapid initial adsorption despite its lower adsorption capacity compared with AB. The substantially lower (qe) value obtained for RT confirms its poor adsorption performance, which is consistent with the experimental adsorption data. Overall, the PFO parameters suggest that adsorption proceeds rapidly during the initial stage owing to the availability of abundant vacant active sites on the biosorbent surface.

The pseudo-second-order model is commonly associated with adsorption processes involving chemisorption, where electron sharing or exchange occurs between adsorbate molecules and surface functional groups. The calculated equilibrium adsorption capacities were 0.394 mol g^{-1} for AB, 0.837 mol g^{-1} for AT, 0.315 mol g^{-1} for RB, and 0.081 mol g^{-1} for RT. The corresponding rate constants ((K2)) were 0.738, 0.021, 0.979, and 0.657 mol^{-1} L min^{-1}, respectively. Raw baobab exhibited the highest (K2) value, indicating a relatively rapid adsorption process once adsorption sites became available. Activated tamarind showed the largest predicted adsorption capacity but the smallest rate constant, implying that adsorption proceeds more slowly but may continue over a longer period before equilibrium is reached. The relatively high (K2) values obtained for AB and RB indicate strong interactions between propionic acid molecules and the active sites generated on the biosorbent surface. The PSO model parameters generally support the possibility that chemical interactions, such as hydrogen bonding and surface complexation between propionic acid molecules and oxygen-containing functional groups on the biosorbents, contribute significantly to the adsorption process.

The Elovich model is widely used to describe heterogeneous adsorption systems and chemisorption processes occurring on energetically diverse surfaces. The initial adsorption rate parameter ((\alpha)) followed the order: AB (0.180) > RB (0.152) > AT (0.044) > RT (0.010) mol g^{-1} min^{-1}. This trend clearly indicates that activated baobab possessed the highest initial adsorption rate, reflecting the abundance of readily accessible adsorption sites created during chemical activation. The desorption constant ((\beta)) values were 9.908, 11.56, 12.50, and 61.30 g mol^{-1} for AB, AT, RB, and RT, respectively. The exceptionally high (\beta) value observed for RT indicates a comparatively greater energy barrier associated with adsorption and suggests a lower surface affinity for propionic acid. In contrast, the lower (\beta) values obtained for AB and AT indicate more favorable adsorption conditions and stronger adsorbate–adsorbent interactions. The Elovich parameters therefore suggest that surface heterogeneity and chemisorption contribute significantly to the adsorption mechanism, particularly for activated biosorbents.

The intraparticle diffusion model was employed to evaluate whether diffusion within the pores of the biosorbents controls the adsorption rate. The intraparticle diffusion rate constants ((K{IPD})) were 11.84, 18.46, 14.70, and 93.45 mol g^{-1} $min^{-1/2}$ for AB, AT, RB, and RT, respectively. Higher values indicate faster diffusion of propionic acid molecules through the adsorbent structure. The intercept parameter ((C)) reflects the contribution of boundary-layer diffusion. Larger positive values indicate a greater influence of external mass-transfer resistance, whereas values close to zero indicate reduced film diffusion effects. The positive intercept observed for AT (0.674 mol g^{-1}) suggests a substantial boundary-layer contribution during adsorption. In contrast, the negative intercepts obtained for AB and RB indicate that intraparticle diffusion alone cannot fully explain the adsorption process and that multiple mechanisms likely operate simultaneously. The small positive intercept for RT further supports the involvement of both surface adsorption and pore diffusion. These findings suggest that adsorption of propionic acid is governed by a combination of external mass transfer, surface adsorption, and intraparticle diffusion rather than by a single rate-controlling mechanism.

The Boyd model was applied to identify whether film diffusion or particle diffusion is the primary rate-limiting step. The Boyd constants ((B)) were determined as 0.259, 0.056, 0.273, and 0.094 min^{-1} for AB, AT, RB, and RT, respectively. Higher (B) values indicate faster transport of adsorbate molecules into the adsorbent particles. Raw baobab exhibited the highest Boyd constant (0.273 min^{-1}), closely followed by activated baobab (0.259 min^{-1}), suggesting relatively rapid diffusion of propionic acid molecules within the particle structure. Activated tamarind displayed the lowest value (0.056 min^{-1}), indicating slower diffusion and supporting the slower adsorption profile observed experimentally. The Boyd constants reveal that diffusion characteristics differ significantly among the biosorbents and are strongly influenced by activation treatment and biomass type.

The kinetic parameters collectively indicate that activated baobab is the most effective biosorbent for propionic acid removal, exhibiting high adsorption capacity, rapid adsorption kinetics, and favorable diffusion characteristics. Raw baobab also demonstrated strong adsorption performance, although activation significantly improved its adsorption efficiency. The Elovich and pseudo-second-order parameters suggest that chemisorption contributes substantially to the adsorption mechanism, while the intraparticle diffusion and Boyd analyses indicate that diffusion processes also influence adsorption rates. Therefore, the adsorption of propionic acid onto the prepared biosorbents is best described as a complex process involving multiple simultaneous mechanisms, including external film diffusion, intraparticle diffusion, and surface chemical interactions. Based on the overall kinetic behavior, the adsorption performance of the biosorbents can be ranked as, AB > RB > AT > RT, which is consistent with the adsorption capacities obtained from the experimental contact-time studies.

Error analytical parameters for kinetic modelling of adsorption of acetic acid using raw and activated baobab and tamarind biosorbents:

Error functions were analyzed, including the sum of squared errors (SSE), mean sum of squared errors (MSSE), standard error (SE), average absolute relative deviation (AARD), and coefficient of determination (R^2) to evaluate the reliability, predictive accuracy, and statistical validity of the kinetic models applied to the adsorption of propionic acid onto raw and activated baobab and tamarind biosorbents (Table 2). The results for pseudo-first-order (PFO), pseudo-second-order (PSO), Elovich (EV), intraparticle diffusion (IPD), and Boyd (BY) models are summarized in Table X. These statistical indicators provide a comprehensive basis for comparing model performance and identifying the most suitable kinetic description of the adsorption process.

Table 2. Error analytical parameters in kinetic modeling of propionic acid using raw and activated baobab and tamarind biosorbents

Model	Error parameters	AB	AT	RB	RT
PFO	SSE	0.2094	0.1027	0.2943	0.0088
	MSSE	0.0233	0.0114	0.0327	0.0010
	SE	0.1525	0.1068	0.1808	0.0313
	AARD	0.5963	0.5234	1.0527	0.4816
	R^2	0.9712	0.9887	0.9857	0.9184
PSO	SSE	0.1031	0.0134	0.2680	0.0230
	MSSE	0.0115	0.0015	0.0298	0.0026
	SE	0.1070	0.0386	0.1726	0.0506
	AARD	0.4246	0.1916	1.0640	0.6603
	R^2	0.9759	0.9907	0.9759	0.9774
EV	SSE	0.1563	0.0581	0.2812	0.0159
	MSSE	0.0174	0.0065	0.0313	0.0018
	SE	0.1298	0.0727	0.1767	0.0410
	AARD	0.5105	0.3575	1.0584	0.5710
	R^2	0.9736	0.9897	0.9808	0.9479
IPD	SSE	0.0115	0.3134	0.3244	0.0346
	MSSE	0.0011	0.0285	0.0295	0.0032
	SE	0.0324	0.1688	0.1717	0.0561
	AARD	0.1095	0.7214	0.8189	0.8531
	R^2	0.9175	0.9243	0.9673	0.8858
BY	SSE	0.0396	0.1255	0.1836	0.0126
	MSSE	0.0043	0.0118	0.0182	0.0012
	SE	0.0615	0.0953	0.1305	0.0275
	AARD	0.1843	0.3897	0.5860	0.3874
	R^2	0.9573	0.9597	0.9764	0.9432

The PFO model shows generally good correlation with experimental data for all biosorbents, with R^2 values ranging from 0.9184 to 0.9887. Among them, activated tamarind (AT) exhibited the highest R^2 value (0.9887), indicating excellent agreement between predicted and experimental adsorption data. AT also showed relatively low error values (SSE = 0.1027, AARD = 0.5234), confirming good predictive performance. Activated baobab (AB) and raw baobab (RB) also demonstrated strong fits, with R^2 values of 0.9712 and 0.9857, respectively. However, RB exhibited comparatively higher error values (AARD = 1.0527), suggesting slightly reduced prediction accuracy. Raw tamarind (RT) showed the weakest fit among all biosorbents (R^2 = 0.9184), indicating that the PFO model is less effective in describing its adsorption behavior compared to the other materials. Overall, the PFO model provides a reasonably good description of the initial adsorption stage but shows variability in predictive accuracy depending on the biosorbent type.

The PSO model demonstrates very strong agreement with experimental data for all biosorbents, with R^2 values ranging from 0.9759 to 0.9907. Activated tamarind (AT) exhibited the best overall fit (R^2 = 0.9907) along with the lowest error metrics (SSE = 0.0134, SE = 0.0386, AARD = 0.1916), indicating highly accurate prediction of adsorption

behavior. Activated baobab (AB) also showed strong performance (R^2 = 0.9759), with relatively low error values, confirming the suitability of the PSO model for describing its adsorption kinetics. Raw baobab (RB) and raw tamarind (RT) showed slightly higher error values but still maintained good agreement with experimental data. The consistently high R^2 values and low error statistics across all biosorbents suggest that the PSO model is the most reliable kinetic model for describing propionic acid adsorption, indicating that chemisorption likely plays a dominant role in the process.

The Elovich model also provides a good fit to the experimental data, with R^2 values ranging from 0.9479 to 0.9897. Activated tamarind (AT) again showed the best agreement (R^2 = 0.9897), followed closely by raw baobab (RB) and activated baobab (AB). Error values for AT were relatively low (SSE = 0.0581, AARD = 0.3575), indicating that adsorption occurs on a heterogeneous surface with varying energy sites. However, raw tamarind (RT) showed comparatively lower performance (R^2 = 0.9479), suggesting less heterogeneity or weaker applicability of this model for untreated biomass. Overall, the Elovich model supports the presence of chemisorption on heterogeneous surfaces, particularly for activated biosorbents.

The IPD model exhibits lower correlation compared to other kinetic models, with R^2 values ranging from 0.8858 to 0.9673. Raw baobab (RB) showed the highest R^2 value (0.9673), suggesting that intraparticle diffusion contributes significantly to its adsorption mechanism. However, the relatively high error values for AT and RT (AARD = 0.7214 and 0.8531, respectively) indicate that diffusion alone does not fully govern the adsorption process. The higher SSE and SE values observed for AT and RB further confirm that multiple mechanisms, rather than intraparticle diffusion alone, control adsorption kinetics. The intercept term obtained in the earlier IPD analysis supports the involvement of boundary layer resistance in the adsorption process. Thus, while intraparticle diffusion plays an important role, it is not the sole rate-limiting step.

The Boyd model provides moderate to good fits, with R^2 values between 0.9432 and 0.9764. Raw baobab (RB) exhibited the highest R^2 (0.9764), followed closely by AT and AB, indicating relatively strong diffusion-controlled behavior in these systems. Activated baobab (AB) and raw tamarind (RT) showed slightly lower R^2 values, suggesting that film diffusion and particle diffusion both influence adsorption rates. The relatively low SSE values across all biosorbents indicate acceptable predictive performance of the model. The Boyd model results suggest that external film diffusion contributes to the overall adsorption rate, but it does not act as the sole controlling mechanism.

A comparative evaluation of all kinetic models based on error analysis and R^2 values indicates the following general order of model suitability: PSO > PFO ≈ Elovich > Boyd > IPD. The pseudo-second-order model consistently shows the best statistical performance across all biosorbents, with the highest R^2 values and the lowest error parameters. This strongly suggests that chemisorption is the dominant mechanism controlling propionic acid adsorption on both raw and activated baobab and tamarind biosorbents. However, the contributions of intraparticle diffusion and film diffusion (as indicated by IPD and Boyd models) confirm that adsorption is not governed by a single mechanism. Instead, the process involves a combination of external mass transfer, pore diffusion, and surface interaction phenomena. Activated biosorbents generally demonstrate better model fitting and lower error values compared with raw materials, confirming that chemical activation enhances surface reactivity, improves adsorption uniformity, and strengthens overall kinetic predictability. In summary, the error analysis validates the robustness of the pseudo-second-order model as the most appropriate descriptor of propionic acid adsorption kinetics and highlights the multi-mechanistic nature of the adsorption process.

4. CONCLUSION

This study investigated the adsorption of propionic acid from aqueous solutions using raw and sulfuric acid–activated biosorbents derived from baobab and tamarind biomass. The results demonstrated that both contact time and biosorbent modification significantly influenced adsorption performance. Activated baobab exhibited the highest adsorption capacity and the fastest uptake rate, followed by raw baobab, activated tamarind, and raw tamarind. This trend confirms that chemical activation enhances surface area, pore development, and the availability of active functional groups, thereby improving adsorption efficiency. Kinetic modeling revealed that adsorption data were best described by the pseudo-second-order model, as indicated by the highest R^2 values and lowest error functions. This suggests that chemisorption, involving surface interactions such as hydrogen bonding and electrostatic attraction, plays a dominant role in propionic acid uptake. Although intraparticle diffusion and film diffusion contributed to the overall process, they were not the sole rate-controlling steps, indicating a multi-mechanistic adsorption system. Error analysis further validated the reliability of the pseudo-second-order model across all biosorbents. Activated materials consistently showed improved model fitting and reduced deviations compared to raw biomass, confirming the effectiveness of activation in enhancing adsorption behavior. Overall, waste-derived baobab and tamarind biosorbents,

particularly in activated form, demonstrate strong potential as low-cost, sustainable adsorbents for the removal of propionic acid from aqueous environments, supporting their application in wastewater treatment systems.

References

1. Afolalu, S. A., Ikumapayi, O. M., Ogedengbe, T. S., Kazeem, R. A., & Ogundipe, A. T. (2022). Waste pollution, wastewater and effluent treatment methods–an overview. Materials Today: Proceedings, 62, 3282-3288.
2. Chapra, S. C., Camacho, L. A., & McBride, G. B. (2021). Impact of global warming on dissolved oxygen and BOD assimilative capacity of the world's rivers: modeling analysis. Water, 13(17), 2408.
3. Tella, T. A., Festus, B., Olaoluwa, T. D., & Oladapo, A. S. (2025). Water and wastewater treatment in developed and developing countries: Present experience and future plans. In Smart Nanomaterials for Environmental Applications (pp. 351-385). Elsevier.
4. Singh, P. K., Kumar, U., Kumar, I., Dwivedi, A., Singh, P., Mishra, S., ... & Sharma, R. K. (2024). Critical review on toxic contaminants in surface water ecosystem: sources, monitoring, and its impact on human health. Environmental Science and Pollution Research, 31(45), 56428-56462.
5. Varriale, L., & Ulber, R. (2023). Fungal-Based Biorefinery: From Renewable Resources to Organic Acids. ChemBioEng Reviews, 10(3), 272-292.
6. Kaur, N., Panesar, P. S., & Ahluwalia, S. (2022). Production of organic acids from agro-industrial waste and their industrial utilization. In Valorization of Agro-Industrial Byproducts (pp. 227-264). CRC Press.
7. Zheng, C., Zhao, L., Zhou, X., Fu, Z., & Li, A. (2013). Treatment technologies for organic wastewater. In Water treatment. IntechOpen.
8. El-Shamy, A. M. (2020). A review on: biocidal activity of some chemical structures and their role in mitigation of microbial corrosion. Egyptian Journal of Chemistry, 63(12), 5251-5267.
9. Ebelegi, A. N., Ayawei, N., & Wankasi, D. (2020). Interpretation of adsorption thermodynamics and kinetics. Open Journal of Physical Chemistry, 10(3), 166-182.
10. Liang, T., Elmaadawy, K., Liu, B., Hu, J., Hou, H., & Yang, J. (2021). Anaerobic fermentation of waste activated sludge for volatile fatty acid production: recent updates of pretreatment methods and the potential effect of humic and nutrients substances. Process Safety and Environmental Protection, 145, 321-339.
11. El Messaoudi, N., Georgin, J., Ciğeroğlu, Z., Şenol, Z. M., Kazan-Kaya, E. S., Arslan, D. Ş., ... & Lacherai, A. (2024). Advanced Physicochemical Techniques for Wastewater Treatment. In Innovative and Hybrid Technologies for Wastewater Treatment and Recycling (pp. 37-77). CRC Press.
12. Fernandes, J., Ramísio, P. J., & Puga, H. (2024). A comprehensive review on various phases of wastewater technologies: Trends and future perspectives. Eng, 5(4), 2633-2661.
13. Crini, G., & Lichtfouse, E. (2019). Advantages and disadvantages of techniques used for wastewater treatment. Environmental chemistry letters, 17(1), 145-155.
14. Meka, U., Kumar, J. A., & Sivamani, S. (2025). Carbon nanomaterials from cassava rhizome for efficient toluene removal from aqueous solutions: Continuous adsorption studies using local and global optimization. South African Journal of Chemical Engineering.
15. Deivasigamani, P., Gajendiran, V., Chitra, B., Kumar, P. S., Balasubramanian, N., Sundararaman, S., ... & Rangasamy, G. (2025). Magnetic Nanoparticles: Synthesis, characterization and application based on environmental Perspective. Results in Chemistry, 102023.
16. Wu, H., Wei, H., Yang, X., Jin, C., Sun, W., Deng, K., ... & Sun, C. (2023). Spherical activated carbons derived from resin-microspheres for the adsorption of acetic acid. Journal of Environmental Chemical Engineering, 11(2), 109394.
17. Hsu, C. F., Chen, Y. T., & Tseng, C. H. (2024). The performance of Adsorbing and Removing gaseous acetic acid by activate carbon. In E3S Web of Conferences (Vol. 530, p. 04002). EDP Sciences.
18. Zabanoot, A. A. M. M., Qatan, A. W. A. S., Hubais, A. S. M., Said, K. H. M. B., & Sivamani, S. (2023). Rejected Lime as Soil Conditioner for Growth of Vigna radiata: A Case Study from Mountainous Ranges of Dhofar Governorate, Oman. Pakistan Journal of Agricultural Research, 36(4), 304-310.
19. Sivamani, S., Nazar, N. A., Krishnan, R. N., & Prasad, B. N. Biogas Production in Dhofar of Oman: Proposed Business Models and SWOT Analysis for Entrepreneurs.
20. Prasad, N., Namdeti, R., Baburao, G., Al-Kathiri, D. S. M. S., Meka, U. R., Tabook, K. M. A., & Joaquin, A. A. (2024). Central composite design for the removal of copper by an Adansonia digitata. Desalination and Water Treatment, 317, 100164.
21. Al-Amri, L., Banerjee, S., Fatima, N., Ramani, S., Vijayasundaram, A., & Sivamani, S (2025). Baobab tree: A review on historical development, ecological importance, cultural significance, and economic potential. GRS Journal of Multidisciplinary Research and Studies, 2(4), 12-20.
22. Malik, V., Saya, L., Gautam, D., Sachdeva, S., Dheer, N., Arya, D. K., ... & Hooda, S. (2022). Review on adsorptive removal of metal ions and dyes from wastewater using tamarind-based bio-composites. Polymer Bulletin, 79(11), 9267-9302.
23. Gajendiran, V., Deivasigamani, P., Sivamani, S., & Sivakumar, P. M. (2023). A review on cassava residues as adsorbents for removal of organic and inorganic contaminants in water and wastewater. Journal of Chemistry, 2023(1), 7891518.

24. Zabanoot, A. A. M. M., Al Amri, F. M. S. I., Al Hamir, H. N. B., Al Hadhri, L. M. A., Al Abd Al-Hadhrami, M. Y., & Sivamani, S. (2025). Adsorption of Hexavalent Chromium on Raw and Activated Cassava Rhizome: Kinetic Analysis Using Mechanistic and Empirical (Regression and ANN) Models. International Journal of Chemical Kinetics, 57(12), 733-743.
25. Qiu, H., Lv, L., Pan, B. C., Zhang, Q. J., Zhang, W. M., & Zhang, Q. X. (2009). Critical review in adsorption kinetic models. Journal of Zhejiang University-Science A, 10(5), 716-724.
26. Musah, M., Azeh, Y., Mathew, J., Umar, M., Abdulhamid, Z., & Muhammad, A. (2022). Adsorption kinetics and isotherm models: a review. Caliphate Journal of Science and Technology, 4(1), 20-26.
27. Revellame, E. D., Fortela, D. L., Sharp, W., Hernandez, R., & Zappi, M. E. (2020). Adsorption kinetic modeling using pseudo-first order and pseudo-second order rate laws: A review. Cleaner Engineering and Technology, 1, 100032.
28. Hu, Q., Pang, S., & Wang, D. (2022). In-depth insights into mathematical characteristics, selection criteria and common mistakes of adsorption kinetic models: A critical review. Separation & Purification Reviews, 51(3), 281-299.
29. Vareda, J. P. (2023). On validity, physical meaning, mechanism insights and regression of adsorption kinetic models. Journal of Molecular Liquids, 376, 121416.
30. Benjelloun, M., Miyah, Y., Evrendilek, G. A., Zerrouq, F., & Lairini, S. (2021). Recent advances in adsorption kinetic models: their application to dye types. Arabian Journal of Chemistry, 14(4), 103031.
31. López-Garzón, C. S., & Straathof, A. J. J. (2014). Recovery of carboxylic acids produced by fermentation. Biotechnology Advances, 32(5), 873–904. https://doi.org/10.1016/j.biotechadv.2014.04.002
32. Fargues, C., Lewandowski, R., Lameloise, M. L., & Decloux, M. (2010). Evaluation of ion-exchange resins for the recovery of organic acids from fermentation broths. Journal of Chemical Technology and Biotechnology, 85, 133–140.
33. Eregowda, T., Rene, E. R., Rintala, J., & Lens, P. N. L. (2020). Volatile fatty acid adsorption on anion exchange resins: kinetics and selective recovery of acetic acid. Separation Science and Technology, 55(8), 1449–1461. https://doi.org/10.1080/01496395.2019.1600553
34. García, V., & King, C. J. (1989). Combined adsorption and ion exchange for carboxylic acid recovery from aqueous streams. Industrial & Engineering Chemistry Research, 28, 863–870.
35. Kawabata, N., Nishiguchi, M., & Seki, H. (1981). Adsorption characteristics of carboxylic acids on weak-base ion-exchange resins. Journal of Applied Polymer Science, 26, 425–435.
36. Pradhan, N., Rene, E. R., Lens, P. N. L., Dipasquale, L., D'Ippolito, G., Fontana, A., Panico, A., & Esposito, G. (2017). Adsorption behaviour of lactic acid on granular activated carbon and anionic resins: Thermodynamics, isotherms and kinetic studies. Energies, 10(5), 665. https://doi.org/10.3390/en10050665
37. Talebi, A., Razali, Y. S., Ismail, N., Rafatullah, M., & Tajarudin, H. A. (2020). Selective adsorption and recovery of volatile fatty acids from fermented landfill leachate by activated carbon process. Science of the Total Environment, 707, 134533. https://doi.org/10.1016/j.scitotenv.2019.134533
38. Reyhanitash, E., Kersten, S. R. A., Schuur, B., & colleagues. (2017). Recovery of volatile fatty acids from fermented wastewater by adsorption. ACS Sustainable Chemistry & Engineering, 5, 9176–9184.
39. Fufachev, A., Mahboubi, A., Taherzadeh, M. J., & co-workers. (2020). Adsorption-based recovery of volatile fatty acids from waste streams: performance and selectivity of adsorbents. Bioresource Technology Reports, 11, 100496.
40. da Silva, C. S., Madeira, L. M., Boaventura, R. A. R., & Costa, C. A. V. (2013). Adsorption/desorption of organic acids onto different adsorbents for their recovery from fermentation broths. Journal of Chemical & Engineering Data, 58(5), 1454–1463. https://doi.org/10.1021/je3008759
41. Sapmaz, T., Mahboubi, A., Taher, M. N., Beler-Baykal, B., Karagunduz, A., Taherzadeh, M. J., & Koseoglu-Imer, D. Y. (2022). Waste-derived volatile fatty acid production and ammonium removal from it by ion exchange process with natural zeolite. Bioengineered, 13, 14751–14769.
42. Wang, S., & Peng, Y. (2010). Natural zeolites as effective adsorbents in water and wastewater treatment. Chemical Engineering Journal, 156, 11–24.
43. Babel, S., & Kurniawan, T. A. (2003). Low-cost adsorbents for heavy metals uptake from contaminated water: A review. Journal of Hazardous Materials, 97, 219–243.
44. Foo, K. Y., & Hameed, B. H. (2010). Insights into the modelling of adsorption isotherm systems. Chemical Engineering Journal, 156, 2–10.
45. Basereh, N., Wainaina, S., Mahboubi, A., & Taherzadeh, M. J. (2025). Fractionation of waste-derived volatile fatty acids by multi-stage adsorption using activated charcoal and Diaion HP-20 resin. Bioengineered, 16, 2458366.
46. Ho, Y. S., & McKay, G. (1999). Pseudo-second-order model for sorption processes. Process Biochemistry, 34, 451–465.
47. Weber, W. J., & Morris, J. C. (1963). Kinetics of adsorption on carbon from solution. Journal of the Sanitary Engineering Division, 89, 31–60.
48. Kyzas, G. Z., & Kostoglou, M. (2014). Green adsorbents for wastewaters: A critical review. Materials, 7, 333–364.
49. Al-Shukaili, S. A., Al-Shukaili, M. A., Al-Baraami, H. A., Al-Mamari, F. S., & Selvaraju, S. (2025). Kinetic modelling for adsorptive removal of acetic acid from its aqueous solution using biosorbents from waste baobab and tamarind of Dhofar. International Journal of Cognitive Computing in Engineering, 6(2), 101-119.